ACS Catalysis

Research Article

pubs.acs.org/acscatalysis

Iron(II) Catalysis in Oxidation of Hydrocarbons with Ozone in Acetonitrile

Hajem Bataineh, Oleg Pestovsky,* and Andreja Bakac*

Ames Laboratory and Chemistry Department, Iowa State University, Ames, Iowa 50011, United States

Supporting Information

ABSTRACT: Oxidation of alcohols, ethers, and sulfoxides by ozone in acetonitrile is catalyzed by submillimolar concentrations of $Fe(CH_3CN)_6^{2+}$. The catalyst provides both rate acceleration and greater selectivity toward the less oxidized products. For example, $Fe(CH_3CN)_6^{2+}$-catalyzed oxidation of benzyl alcohol yields benzaldehyde almost exclusively (>95%), whereas the uncatalyzed reaction generates a 1:1 mixture of benzaldehyde and benzoic acid. Similarly, aliphatic alcohols are oxidized to aldehydes/ketones, cyclobutanol to cyclobutanone, and diethyl ether to a 1:1 mixture of ethanol and acetaldehyde. The kinetics of oxidation of alcohols and diethyl ether are first-order in $[Fe(CH_3CN)_6^{2+}]$ and $[O_3]$ and independent of [substrate] at concentrations greater than ~5 mM. In this regime, the rate constant for all of the alcohols is approximately the same, $k_{cat} = (8 \pm 1) \times 10^4\ M^{-1}\ s^{-1}$, and that for $(C_2H_5)_2O$ is $(5 \pm 0.5) \times 10^4\ M^{-1}\ s^{-1}$. In the absence of substrate, $Fe(CH_3CN)_6^{2+}$ reacts with O_3 with $k_{Fe} = (9.3 \pm 0.3) \times 10^4\ M^{-1}\ s^{-1}$. The similarity between the rate constants k_{Fe} and k_{cat} strongly argues for $Fe(CH_3CN)_6^{2+}/O_3$ reaction as rate-determining in catalytic oxidation. The active oxidant produced in $Fe(CH_3CN)_6^{2+}/O_3$ reaction is suggested to be an Fe(IV) species in analogy with a related intermediate in aqueous solutions. This assignment is supported by the similarity in kinetic isotope effects and relative reactivities of the two species toward substrates.

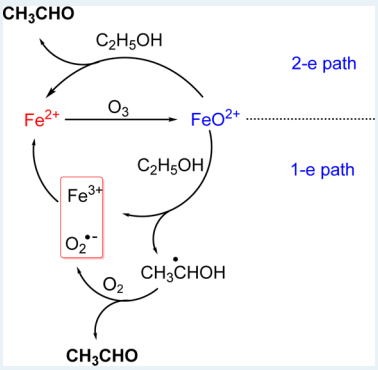

KEYWORDS: *iron, ozone, oxidation, catalysis, alcohol, kinetics, mechanism*

INTRODUCTION

Previous studies from this group[1,2] and others[3,4] have established that the reaction of $Fe(H_2O)_6^{2+}$ with ozone generates an iron(IV) species best described as $Fe^{IV}(H_2O)_5O^{2+}$ (hereafter $Fe_{aq}O^{2+}$) on the basis of spectroscopic evidence, conductivity measurements, chemical reactivity, and DFT calculations.[1,2,5] Oxidations with this high-spin Fe(IV) complex take place by oxygen atom transfer to, for example, sulfoxides and phosphines and by hydride and hydrogen atom abstraction from C−H bonds.[1] In reactions with alcohols, aldehydes and ethers, the latter two mechanisms operate in parallel (Scheme 1). The hydride path is catalytic as it generates $Fe(H_2O)_6^{2+}$, which can be reoxidized to $Fe_{aq}O^{2+}$. Overall, however, the catalytic efficiency is poor because of the loss of iron as $Fe(H_2O)_6^{3+}$ in the parallel one-electron (hydrogen atom transfer) path.

In the reaction between $Fe(H_2O)_6^{2+}$ and H_2O_2 (Fenton reaction), the reactive intermediate changes from hydroxyl radicals in acidic solutions to an iron(IV) species at near neutral pH.[6] Such a major mechanistic change caused by a modest change in reaction conditions led us to consider the effect of other parameters, including solvent, on reactions involving solvento iron species in oxidation states 2+ to 4+. Specifically, the much higher reduction potential of the Fe(III)/Fe(II) couple in acetonitrile[7,8] as compared with that in water suggests that the preference for two-electron pathways of a hypothetical iron(IV) species might be greater in acetonitrile. To explore this possibility and its potential consequences for iron-catalyzed oxidations, we initiated a study of the reaction of Fe(II) with O_3 in acetonitrile in the presence of oxidizable substrates.[9] The results are described herein.

Scheme 1

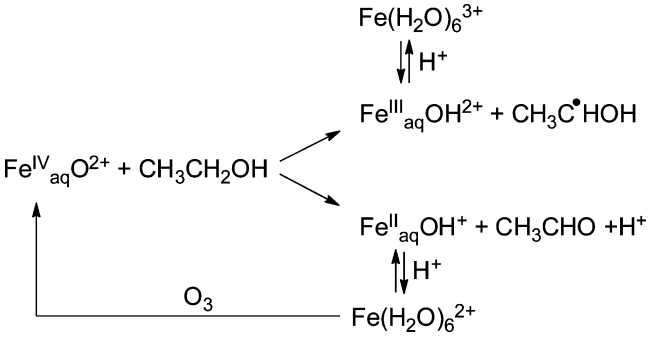

EXPERIMENTAL SECTION

The following chemicals were obtained commercially and used as received: iron(II) perchlorate hydrate $Fe(ClO_4)_2 \cdot xH_2O$

Received: December 8, 2014
Revised: January 27, 2015
Published: January 29, 2015

DOI: 10.1021/cs501962m
ACS Catal. 2015, 5, 1629−1637

(98%), deuterium oxide D_2O (99.9 atom % D), 1,10-phenanthroline (99+%), benzyl alcohol anhydrous (99.8%), cyclobutanol (99+%) (all Aldrich); dimethyl sulfoxide (≥99.9%, ACS spectrophotometric grade) and cyclopentanol (99%) (both Sigma-Aldrich); 2-propanol (99.9% certified ACS), tetrahydrofuran (99.9% HPLC grade), and ethyl ether anhydrous (99.9% certified ACS) (all Fisher scientific); acetonitrile-d_3 (99.8 atom % D) (Cambridge Isotope Laboratories, Inc.); acetonitrile (low water content (~10 ppm) for HPLC, GC, and spectrophotometry, Honeywell-Burdick & Jackson); 2-propanol-2-d_1 (99.8 atom % D) and 2-propanol-d8 (99.9 atom % D) (both CDN Isotopes); and benzyl-α,α-d_2 alcohol (98 atom % D, ISOTEC). Iron(II) bis(acetonitrile)bis(triflate), $Fe(CF_3SO_3)_2(CH_3CN)_2$, was synthesized according to a literature procedure.[10] The solution species in acetonitrile is assumed to be $Fe(CH_3CN)_6^{2+}$, and this formula is used throughout the paper, although small amounts of mixed acetonitrile−water complexes cannot be ruled out. This is especially true for experiments with added water.

In experiments designed to explore the effect of water on products and kinetics, anhydrous iron(II) triflate was used instead of hydrated iron(II) perchlorate. Deuterated acetonitrile was dried over 4A molecular sieves until the HDO/H_2O signal disappeared in the ^1H NMR spectrum. The water content at that point is estimated at <40 μM, the minimum amount required for an observable NMR signal under our conditions. More rigorous efforts at achieving strictly anhydrous conditions were not pursued, given that most of the reactions in this work generate water as one of the products in amounts much greater (up to several millimolar) than those potentially introduced with our solvents and reagents. Moreover, as shown later, up to 100 mM of externally added water has no effect on product yields or catalyst recovery, and kinetics are affected only mildly at >50 mM water.

UV−vis absorbance measurements and kinetic studies used a Shimadzu UV-3101 PC spectrophotometer and Olis RSM-1000 stopped-flow at 24.9 ± 0.1 °C. ^1H NMR spectra were recorded with a 400 MHz Bruker DRX-400 or 600 MHz Bruker Avance III spectrometer at room temperature. A Waters GCT accurate mass time-of-flight mass spectrometer in positive EI mode (70 EV) with a scan rate of 0.3 s per scan and a mass range of 10−200 Da were used to qualitatively detect some of the products. Waters MassLynx 4.0 software was used to acquire and process GC/MS data. Ozone was generated in an Ozonology L-100 ozone generator. The oxygen concentration was measured using a Hanna Edge dissolved oxygen meter.

Procedures. Stock solutions of iron(II) perchlorate in CH_3CN or CD_3CN were prepared fresh before each set of experiments and standardized with phenanthroline after dilution with H_2O and using $\varepsilon = 1.14 \times 10^4$ M^{-1} cm^{-1}. No $Fe(phen)_3^{3+}$ was detected in these solutions. Determinations of Fe(II) concentrations in spent reaction solutions utilized a correction for Fe(III) as previously described.[1] Ozone solutions were prepared by continuous bubbling of ozone through CH_3CN or CD_3CN for >5 min at room temperature and diluted to the desired concentration. The concentration of ozone in the stock solutions was typically 5.6 ± 0.1 mM, as determined spectrophotometrically at 260 nm, $\varepsilon_{260} = 3350$ M^{-1} cm^{-1}. These solutions always contained residual oxygen, typically ~5.9 mM, as described below.

To determine the amount of oxygen generated in the $Fe(CH_3CN)_6^{2+}/O_3$ reaction in the presence and absence of substrates, the reactants were mixed rapidly in an air-free, tightly sealed vial, leaving only minimal head space to avoid equilibration between the solution and gas phases. A sample (0.5−1.0 mL) was withdrawn and injected into another sealed vial containing a dissolved oxygen electrode immersed in 18 mL of air-free water. The measurement was completed in ~40 s after injection. The measured value was corrected for the concentration of residual oxygen, typically around 5.9 mM in ozone stock solutions as determined after removal of O_3 with excess fumaric or maleic acid.[11] The same procedure was used to determine the concentration of O_2 in O_2-saturated acetonitrile. The value obtained, 11.3 mM, is in acceptable agreement with the value reported for air-saturated acetonitrile, 2.42 mM.[12]

Except in experiments specifically designed to explore the effect of O_2 on kinetics and products, solutions of iron(II) and substrates were prepared and handled anaerobically. However, because some O_2 was present in the stock solutions of ozone (see above) and because the $Fe(CH_3CN)_6^{2+}/O_3$ reaction itself produces O_2, none of the reaction solutions were completely O_2-free.

Competition Experiments and Product Analysis. A solution containing known concentrations of Fe(II) and two or three substrates were mixed with ozone in a UV cell. After the disappearance of ozone (absorbance at 260 nm), the products were quantified by ^1H NMR. In all of the experiments, the substrate concentrations were sufficiently large to make the kinetics of each individual reaction fall into the plateau region (see Results). Product yields for benzyl alcohol, which absorbs too strongly in the UV for direct kinetic measurements, were shown independently to remain unchanged at $[PhCH_2OH]_0 \geq 4$ mM. Similar experiments were conducted on mixtures of protiated and fully or partially deuterated substrates to determine kinetic isotope effects. Product yields derived from fully deuterated substrates (diethyl ether-d_{10} and 2-propanol-d_8) were estimated as a difference between the total amount of products for the same competition observed with protiated compounds and the amount of product derived from the competing protiated substrate.

Catalyst concentrations in product analysis experiments (Tables 1−7) were chosen so as to minimize the contribution from uncatalyzed O_3/substrate reaction. Typically, >95% of the reaction proceeded by the catalyzed path, except in experiments with 2-propanol (Tables 1 and 3) in which the uncatalyzed path contributed 16% and 10%, respectively.

Kinetic data were obtained by monitoring the disappearance of ozone at 260 nm (Shimadzu) or in the 260−280 nm spectral

Table 1. Product Yields in $Fe(CH_3CN)_6^{2+}$-Catalyzed Oxidation of Alcohols, DMSO, and Et_2O by Ozone

substrate (mM)	$[O_3]$ (mM)	$[Fe(CH_3CN)_6^{2+}]$ (mM)	major product	% yield
dimethyl sulfoxide (9.6)	1.9	0.028	dimethyl sulfone	100
diethyl ether (8.5)	1.2	0.052	(ethanol + acetaldehyde)	100
cyclopentanol (9.8)	1.4	0.024	cyclopentanone	85
cyclobutanol (9.6)	1.8	0.025	cyclobutanone	85
2-propanol (32)	0.1	0.025	acetone	80
ethanol (21.1)	0.83	0.055	acetaldehyde	70
benzyl alcohol (10)	1.8	0.048	benzaldehyde	70

DOI: 10.1021/cs501962m
ACS Catal. 2015, 5, 1629−1637

range (Olis RSM-1000 Rapid Scan). In stopped flow experiments, a mixture of $Fe(CH_3CN)_6^{2+}$ and substrate was placed in one syringe, and ozone, in the other. Experiments designed to study the effect of [substrate] used 0.06−0.15 mM ozone, 0.025 mM $Fe(CH_3CN)_6^{2+}$, and 1−50 mM substrate. The effect of $[Fe(CH_3CN)_6^{2+}]$ was explored at 0.08−0.12 mM ozone, 0.005−0.1 mM $Fe(CH_3CN)_6^{2+}$, and 2−50 mM substrate.

Kinetic traces were fitted to an expression for first-order kinetics with Kaleidagraph v4.0 or with OLIS Global-Works v2.0.190. ^{1}H NMR and GC/MS analyses were initiated within 5−15 min after completion of the reaction. 10% D_2O (v/v) was added to some NMR solutions to shift the interfering water peak.

RESULTS

The UV spectrum after completion of the reaction between 1.1 mM benzyl alcohol and 0.22 mM ozone in acetonitrile exhibits a double feature in the 230−250 nm range, (Figure 1) that is consistent with a mixture of benzaldehyde (λ_{max} 244 nm) and benzoic acid (λ_{max} 227 nm). The individual spectra are shown in Figure S1. This assignment was confirmed by ^{1}H NMR (Figure S2). The reaction also produced hydrogen peroxide, as shown by ^{1}H NMR signal at 8.56 ppm.

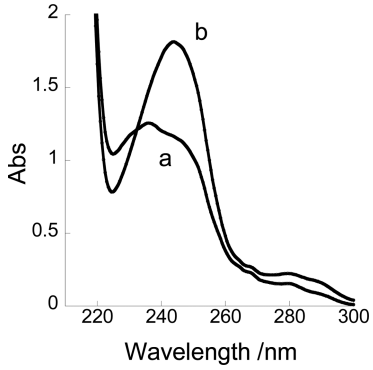

Figure 1. UV spectra of the products of the reaction between (a) 1.1 mM $PhCH_2OH$ and 0.22 mM O_3, and (b) 1.1 mM $PhCH_2OH$ and 0.3 mM O_3/0.011 mM $Fe(CH_3CN)_6^{2+}$.

When the same reaction was conducted in the presence of 0.011 mM $Fe(CH_3CN)_6^{2+}$, benzaldehyde was the major product detected by UV (Figure 1), ^{1}H NMR (Figure S2), and GC/MS. Small amounts of benzoic acid (∼10%) were also observed, some of it possibly generated by oxidation of benzaldehyde with O_2 during sample manipulation. The combined yield of PhCHO and PhCOOH, based on initial ozone concentration, was 85%.

$Fe(CH_3CN)_6^{2+}$-catalyzed oxidation of cyclobutanol by O_3 (1.8 mM) produced 1.55 mM cyclobutanone (Figure S3). No ring-opened products were observed by either ^{1}H NMR or GC/MS, ruling out a significant contribution from a path involving cyclobutanol radicals.[1] The latter are subject to rapid ring opening that ultimately yields an aldehyde(s). At the end of the reaction, ∼80% of iron was still present as Fe(II).

Similarly, ethanol was oxidized to acetaldehyde (Figure S4), 2-propanol to acetone, and cyclopentanol to cyclopentanone. The results are summarized in Table 1. Product yields varied from 70% (acetaldehyde) to 85% (cyclopentanone). ^{1}H NMR of the products of ethanol oxidation exhibits additional signals at 8.03 and 4.64 ppm, consistent with small amounts of formic acid and acetal, which are common overoxidation products of ethanol.[13] The yields of these products increase somewhat with increasing $[O_3]/[EtOH]$ ratio.

The reaction with diethyl ether produced a 1:1 mixture of C_2H_5OH and CH_3CHO in 100% yield (Figure S5). Dimethyl sulfoxide (DMSO) was oxidized to the sulfone, also in 100% yield (Figure S6). At an initial $Fe(CH_3CN)_6^{2+}$ concentration of >0.020 mM, the majority (70−90%) of iron was still present as Fe(II) at the end of the reactions listed in Table 1, provided the concentration of the substrate exceeded ∼5 mM. At much lower initial concentrations of $Fe(CH_3CN)_6^{2+}$ and substrate, up to 40−60% of $Fe(CH_3CN)_6^{2+}$ was oxidized to Fe(III).

$Fe(CH_3CN)_6^{2+}$-catalyzed oxidation of THF by O_3 yielded several products, as shown by GC/MS and ^{1}H NMR (Figures 2 and S7). On the basis of mass spectra, the GC peak at 4.42 min is assigned to an equilibrated mixture[14] of 2-hydroxytetrahydrofuran (2-OH-THF) and 4-hydroxybutanal, and that at 6.18 min, to γ-butyrolactone. All three species were clearly identified and quantified by ^{1}H NMR (Figure S7). The combined yield is 75% (in 4:2:1 ratio, respectively). Also observed in ^{1}H NMR are small amounts of formic acid, which was also found in previous studies of THF oxidation.[15] Several other small NMR peaks and the GC peak at 4.95 min in Figure 2 were not identified. The corresponding GC peak was also observed and remained unidentified in an earlier study of THF oxidation.[15] The products eluting at 9−10 min in Figure 2 are attributed to THF dimers and condensation products as deduced from mass

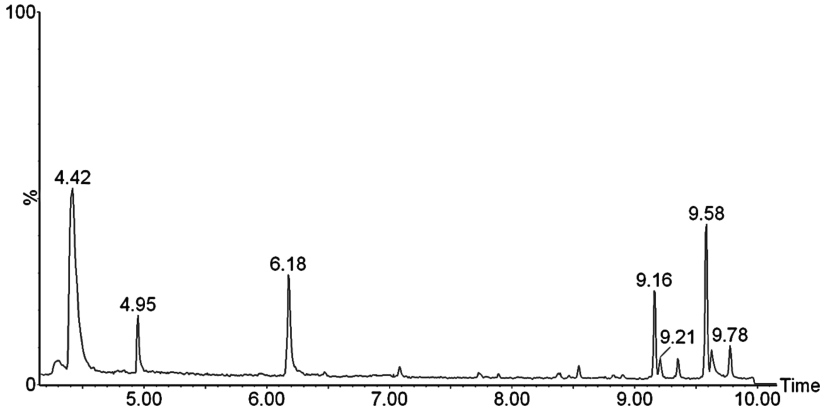

Figure 2. Gas chromatogram of products obtained by oxidation of 5.6 mM THF by 1.35 mM O_3/0.1 mM Fe(II).

DOI: 10.1021/cs501962m
ACS Catal. 2015, 5, 1629−1637

spectral data. These products are also formed upon electrochemical oxidation of THF in aqueous sulfuric acid.[15]

The overall picture of THF oxidation changes dramatically when an alcohol is added as cosubstrate. As shown on the example of THF/benzyl alcohol mixture (Figures S8–S10), the main products (>90%) are the acetal 2-OR-THF and aldehyde/ketone derived from the alcohol. THF oxidation products, that is, hydroxytetrahydrofuran/4-hydroxybutanal and γ-butyrolactone, accounted for only 5% of products.

In search of the source of 2-OR-THF, we considered the known reaction[16] between alcohols and 4-hydroxybutanal, the latter being one of THF oxidation products. This reaction generates 2-OR-THF in the presence of an acid catalyst at 20–100 °C,[16] but is extremely slow (about 17 h) under our experimental conditions. In addition, no new products were generated upon mixing alcohols with product solutions of $Fe(CH_3CN)_6^{2+}/O_3$/THF reaction. A slow overnight reaction between alcohols and THF in the presence of $Fe(CH_3CN)_6^{2+}$ (0.5 mM) did produce 2-OR-THF when the concentrations of alcohols (60 mM) and THF (80 mM) were about 10-fold higher than is typical in our work. Clearly, the rapid (several seconds) formation of 2-OR-THF under our standard catalytic conditions utilizes a different path and must involve an intermediate(s) generated in the course of the $Fe(CH_3CN)_6^{2+}/O_3$ oxidation of THF or alcohol. Because close to 100% of iron was still present as Fe(II) at the end of the $Fe(CH_3CN)_6^{2+}/O_3$/THF/alcohol reaction, either the products were formed in a series of 2-e steps or Fe(III), if involved, was rereduced to Fe(II) by reaction intermediate(s).

Kinetics. Substrates (5–50 mM) were used in large excess over ozone (0.06–0.15 mM) and $Fe(CH_3CN)_6^{2+}$. The loss of ozone was monitored at 260 nm. Kinetic traces in the plateau region (see below) were exponential and yielded pseudo-first-order rate constants, k_{obs}.

Ozone oxidation of organic substrates used in this work is slow but not negligible in comparison with the $Fe(CH_3CN)_6^{2+}$-catalyzed reaction. The rate law for the disappearance of ozone is thus given by eq 1, where k_{cat} represents the rate constant for the catalytic reaction of eq 2, k_{O_3} is the independently determined rate constant for the direct O_3/substrate reaction (Table S1), and S is substrate. The contribution from direct reaction to k_{obs} was typically <10%, but increased as substrate concentrations increased and Fe(II) concentrations decreased. In the least favorable case (30 mM 2-PrOH at 0.025 mM Fe(II)), this contribution was 16%. The use of higher concentrations of the catalyst, which would benefit catalytic reaction, was not feasible because the kinetics became too fast and signal-to-noise ratio was poor.

$$-d[O_3]/dt = k_{O_3}[O_3][S] + k_{cat}[O_3]\,[Fe(CH_3CN)_6^{2+}]^m[S]^n = k_{obs}[O_3] \quad (1)$$

$$O_3 + S \xrightarrow{[Fe(II)}} \text{products} \quad k_{cat} \quad (2)$$

The experimentally determined k_{obs} was corrected for the direct path to give k_{corr}, eq 3.

$$k_{corr} = k_{obs} - k_{O_3}[S] = k_{cat}[Fe(CH_3CN)_6^{2+}]^m[S]^n \quad (3)$$

The reaction is first-order in $[Fe(CH_3CN)_6^{2+}]$ ($m = 1$) as shown by linear dependence of k_{corr} on $[Fe(CH_3CN)_6^{2+}]$ at two different concentrations of 2-PrOH in Figure 3. First-order dependence on $[Fe(CH_3CN)_6^{2+}]$ holds for all of the substrates examined. Identical results were obtained with $Fe(ClO_4)_2 \cdot xH_2O$ and $Fe(CF_3SO_3)_2(CH_3CN)_2$ as the source of $Fe(CH_3CN)_6^{2+}$.

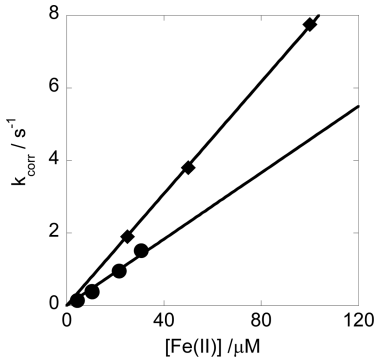

Figure 3. Plot of k_{corr} vs concentration of $Fe(CH_3CN)_6^{2+}$ for the catalytic oxidation of 2-PrOH with ozone (0.08–0.12 mM.). Concentrations of 2-PrOH are 2 mM (circles) and 50 mM (squares).

The dependence on [2-PrOH], on the other hand, is quite modest, as shown by the small difference in the slopes of the two lines in Figure 3, that is, 3.6×10^4 M^{-1} s^{-1} and 7.7×10^4 at [2-PrOH] = 2 mM and 50 mM, respectively. This general picture also holds for other substrates, as shown in Table S2 and illustrated by the plot of k_{corr} vs [Substrate] in Figure 4.

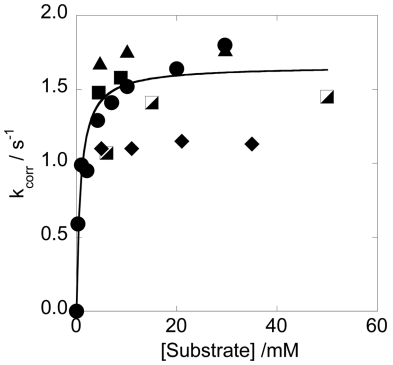

Figure 4. Plot of k_{corr} against substrate concentration for $Fe(CH_3CN)_6^{2+}$-catalyzed oxidations with ozone of 2-propanol (●), ethanol (◪), THF (■), cyclobutanol (▲) and diethyl ether (◆). All experiments have $[Fe(CH_3CN)_6^{2+}]_0$ = 0.025 mM, $[O_3]$ = 0.06–0.15 mM.

After the sharp initial rise, the rate constants in Figure 4 reach an approximately constant value of 1.5 ± 0.2 s^{-1} for most substrates and 1.1 s^{-1} for diethyl ether. The initial concentration of $Fe(CH_3CN)_6^{2+}$ in these experiments was approximately constant at 0.025 ± 0.002 mM. After the reaction, ~80% of $Fe(CH_3CN)_6^{2+}$ was recovered in the plateau region in Figure 4, but only ~50% in the rising portion at low substrate concentrations. In addition, the fit to exponential kinetics at low [substrate] was poor, and only the initial 50% of the reaction was used to evaluate the rate constants.

In the plateau region, the reaction is clearly catalytic in $Fe(CH_3CN)_6^{2+}$, and the rate law is reasonably well approximated by eq 4 (i.e., n of eq 3 is 0), yielding $k_{cat} = k_{corr}/[Fe(CH_3CN)_6^{2+}] = (5 \pm 0.5) \times 10^4$ M^{-1} s^{-1} for Et_2O and $(8 \pm 1) \times 10^4$ M^{-1} s^{-1} for the remaining substrates.

DOI: 10.1021/cs501962m
ACS Catal. 2015, 5, 1629–1637

$$-d[O_3]/dt = d[\text{product}]/dt = k_{cat}[Fe(CH_3CN)_6^{2+}][O_3] = k_{corr}[O_3] \quad (4)$$

The results for 2-propanol deviate somewhat from this picture in that the rate constant continues to increase slowly with increasing [2-propanol]. Of all the aliphatic alcohols studied, 2-propanol is the most reactive in the direct reaction with O_3 (Table S1) so that the correction for this term becomes significant at higher concentrations of 2-PrOH, as already commented. Under these conditions, the two pathways may not remain completely independent, that is, intermediates from one may cross over to the other and lead to the observed increase in rate constant. The proportion of the direct pathway can be minimized experimentally by increasing the catalyst concentration and enhancing the catalytic path. Such conditions were used in product analysis, but for kinetic studies, this option is not feasible because the increased rate of the catalytic component made the overall reaction too fast to monitor.

The kinetic behavior of DMSO is qualitatively similar to that of alcohols and ethers, but the rate constant is much larger, reaching an (extrapolated) saturation value of 39 ± 1 s^{-1} at 0.025 mM Fe(II) (Figure 5). This result implies much greater

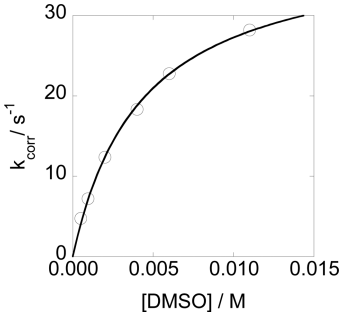

Figure 5. Plot of k_{obs} vs [DMSO] for the reaction with O_3 (0.1 mM)/$Fe(CH_3CN)_6^{2+}$ (0.025 mM).

reactivity of the $Fe(DMSO)_n(CH_3CN)_{6-n}^{2+}$ complex(es)[17,18] compared with $Fe(CH_3CN)_6^{2+}$. The support for $Fe(DMSO)_n(CH_3CN)_{6-n}^{2+}$ in this work comes from the observation of broadened ^1H NMR methyl resonances of DMSO in CD_3CN in the presence of Fe(II), which is consistent with an exchange between free and complexed DMSO. As expected, the signal sharpens upon addition of D_2O, which leads to dissociation of DMSO.

Kinetic measurements for the $Fe(CH_3CN)_6^{2+}/O_3$ reaction in the absence of substrates and with $Fe(CH_3CN)_6^{2+}$ in large excess yielded k_{obs} = 20 s^{-1} at $[Fe(CH_3CN)_6^{2+}]_0$ = 0.21 mM and 29 s^{-1} at $[Fe(CH_3CN)_6^{2+}]_0$ = 0.30 mM, which results in $k_{Fe} = (9.3 \pm 0.3) \times 10^4$ M^{-1} s^{-1} (eq 5). The similarity between the rate constants k_{Fe} and k_{cat} strongly argues that they apply to the same reaction, that is, formation of an intermediate, presumably $Fe^{IV}(CH_3CN)_5O^{2+}$ (hereafter, $Fe^{IV}_{AN}O^{2+}$; see later) or a related species in analogy with $Fe^{IV}_{aq}O^{2+}$ that is produced in the $Fe(H_2O)_6^{2+}/O_3$ reaction in acidic aqueous solutions.[1] In this scenario, $Fe^{IV}_{AN}O^{2+}$ rapidly oxidizes substrates as in eq 6, thereby regenerating $Fe(CH_3CN)_6^{2+}$ which re-enters eq 5.

$$Fe(CH_3CN)_6^{2+} + O_3 \rightarrow Fe^{IV}(CH_3CN)_5O^{2+} + O_2 + CH_3CN \quad k_{Fe} \quad (5)$$

$$Fe^{IV}(CH_3CN)_5O^{2+} + (C_2H_5)_2O \xrightarrow{CH_3CN,fast} Fe(CH_3CN)_6^{2+} + \{C_2H_5OH + CH_3CHO\} \quad (6)$$

Runs with excess ozone exhibited a rapid initial step, followed by slower disappearance of large, nonstoichiometric amounts of ozone in a reaction apparently catalyzed by iron. The fast initial step took place on a time scale appropriate for k_{Fe} that was determined with excess $Fe(CH_3CN)_6^{2+}$, but a reliable rate constant could not be extracted under those conditions.

In several experiments, the concentration of O_2 was determined at the end of reaction with use of dissolved oxygen electrode as described in the Experimental Section. Under standard catalytic conditions (0.050 mM $Fe(CH_3CN)_6^{2+}$, 0.8 mM O_3, 20 mM substrate), the reactions with DMSO and with $(C_2H_5)_2O$ generated 0.9 equiv of O_2 per O_3 (Table S3). This result, combined with quantitative product yields in Table 1, leads to the approximate stoichiometry in eq 7.

$$O_3 + (C_2H_5)_2O(\text{or } Me_2SO) \xrightarrow{Fe(II)} \{CH_3CHO + C_2H_5OH\}(\text{or } Me_2SO_2) + O_2 \quad (7)$$

For the remaining substrates in Table 1, the net increase in O_2 content was lower, typically 0.6 equiv per O_3, suggesting some O_2 consumption in parallel 1-e processes (see below). When no substrates were added, the increase in O_2 was only ~0.2 equiv per mole of O_3, regardless of whether $Fe(CH_3CN)_6^{2+}$ was used in catalytic amounts or in concentrations comparable to those of O_3 (~0.8 mM). In both cases, ozone was consumed completely, although at low iron concentrations, the reaction took ~15 min, much longer than in the presence of added substrates. Given that O_3 persists in acetonitrile for hours in the absence of $Fe(CH_3CN)_6^{2+}$, it is clear that $Fe(CH_3CN)_6^{2+}$/acetonitrile combination leads to catalytic O_3 consumption, although acetonitrile is less reactive than the substrates in Table 1. Moreover, small amounts of $Fe(CH_3CN)_6^{2+}$ remained after completion of the reaction, even when ozone was in excess. In experiments with equimolar amounts of $Fe(CH_3CN)_6^{2+}$ and O_3, ~60% of Fe(II) remained after completion of the reaction in CH_3CN, but only traces (<5%) in CD_3CN, demonstrating a large solvent kie. Unfortunately, no oxidation products of CH_3CN could be detected by ^1H NMR or GC/MS owing to interference by the large solvent peaks. No formaldehyde was detected with chromotropic acid.

Effect of Fe(III), O_2 and Water. There is a mild increase in product yields under oxygen-rich conditions, as shown for ethanol in Table 2. At approximately constant concentrations of $Fe(CH_3CN)_6^{2+}$, O_3, and EtOH, an increase in oxygen concentration from 1 to 7 mM led to an increase in acetaldehyde yield from 82% to 94% and an increase in the recovery of $Fe(CH_3CN)_6^{2+}$ from 91% to 98%. Oxygen also appears to have a mild inhibiting effect on the kinetics. The rate constant in the presence of excess O_2 (≥1.3 mM) is ~15% smaller than that obtained in the experiments that had only a small background concentration of O_2 (~0.2 mM, comparable to that of ozone).

DOI: 10.1021/cs501962m
ACS Catal. 2015, 5, 1629−1637

Table 2. Effect of Fe(III) and O_2 on Ethanol Oxidation[a]

$[O_2]$ (mM)	$[Fe(III)]_0$ (mM)	% $[CH_3CHO]_\infty$[b]	% $[Fe(II)]_\infty$[c]
1		82	91
1[d]		82	93
7		94	98
1	0.052	85	105
1	0.24	100	130

[a] $[Fe(CH_3CN)_6^{2+}]_0$ = 0.047−0.060 mM, $[O_3]$ = 0.93−1.0 mM, $[C_2H_5OH]$ = 43−55 mM. [b] Percent yield of CH_3CHO. [c] Percent Fe(II) recovered after reaction. [d] Added $[H_2O]$ = 56 mM.

Externally added $Fe(ClO_4)_3$ also improves product yields. As shown in the last entry in Table 2, the yields of acetaldehyde become quantitative in the presence of 0.24 mM Fe(III).

Replacing the Fe(II) catalyst with Fe(III) results in a slow initial decrease in ozone concentration, but the reaction accelerates with time, suggesting a buildup of Fe(II) and onset of Fe(II) catalysis. Experiments with Fe(III)/EtOH/acetonitrile confirmed that Fe(II) was, indeed, produced.

Up to 100 mM of added water has no effect on the product yields or catalyst recovery, as shown for ethanol and 2-propanol in Tables 2 and 3, but the rate constant shows a small

Table 3. Effect of H_2O on the Kinetics and Catalyst Recovery[a]

$[O_3]$ (mM)	substrate	added $[H_2O]$ (mM)	k_{corr} (s^{-1})	% $[Fe(II)]_\infty$[b]
0.054	2-propanol	0	1.7	96
0.064	2-propanol	50	2.0	92
0.056	2-propanol	99	2.6	96
0.050	2-propanol	198	3.0	80
0.072	ethanol	0	1.4	92
0.063	ethanol	149	2.3	76
0.060	ethanol	489	4.4	64

[a] Conditions: [substrate] = 20 mM, $[Fe(CH_3CN)_6^{2+}]_0$ = 0.025 mM. [b] Percentage of Fe(II) recovered after reaction.

systematic increase with increasing $[H_2O]$. At larger concentrations of H_2O, both product yields and catalyst recovery decrease, and the rate constant increases. All catalytic activity ceases when the water content reaches 3% (~1.5 M). The presence of water in the coordination sphere of iron and in the solvent apparently changes the Fe(III)/Fe(II) potentials to an extent sufficient to restore the chemistry to that characteristic of aqueous solution.[1]

Competition Experiments. Because the $Fe(CH_3CN)_6^{2+}/O_3$ reaction is rate-determining, direct kinetic measurements do not provide information on the reactivity of catalytic intermediate(s). To obtain some insight into the relative reactivity of $Fe^{IV}_{AN}O^{2+}$ toward various substrates and to determine kinetic isotope effects, competition experiments were performed (see the Experimental Section). The results (Figures S11−S16) are summarized in Tables 4−7. The ratios of rate constants k_1/k_2 for various substrates were calculated from the expression $k_1/k_2 = [P_1][S_2]/[P_2][S_1]$, where S_1 and S_2 are two competing substrates, and P_1 and P_2 their respective products. In the experiment with three competing substrates, the listed ratios are $[P_1][S_2]/[P_2][S_1]$ and $[P_2][S_3]/[P_3][S_2]$, where S_3 and P_3 stand for $(CH_3)_2CHOH$ and $(CH_3)_2CO$, respectively. No corrections were applied for different numbers of abstractable hydrogens in different substrates.

Table 4. Results of Competition Experiments[a]

O_3 (mM)	substrate (mM)	product (mM)	k_1/k_2[b]
0.66	benzyl alcohol (4.9) + ethanol (19)	benzaldehyde (0.27) + acetaldehyde (0.25)	4.2
0.73	benzyl alcohol (4.9) + cyclobutanol (10)	benzaldehyde (0.29) + cyclobutanone (0.31)	1.9
1.7	cyclobutanol (10) + ethanol (30)	cyclobutanone (0.62) + acetaldehyde (0.76)	2.4
0.86	cyclobutanol (10) + 2-propanol (11)	cyclobutanone (0.40) + acetone (0.34)	1.3
1.0	benzyl alcohol (4.7) + ethanol (10) + 2-propanol (9.6)	benzaldehyde (0.32) + acetaldehyde (0.18) + acetone (0.32)	3.8, 0.54[c]
1.1	benzyl alcohol (4.8) + diethyl ether (4.7)	benzaldehyde (0.49) + acetaldehyde/ethanol (0.37)	1.3

[a] $[Fe(CH_3CN)_6]$ = 0.05−0.06 mM. [b] Ratio of rate constants for competing substrates S_1 and S_2 in the order listed in each set. [c] Ratio of rate constants for ethanol and 2-propanol.

Table 5. Relative Rate Constants for Oxidations with $Fe^{IV}_{AN}O^{2+}$

substrate	av k_{rel}	k_{H_2O} (M^{-1} s^{-1})[a]
ethanol	[1.0]	2.51×10^3
2-propanol	2.0	3.22×10^3
cyclobutanol	2.2	3.13×10^3
diethyl ether	3.1	4.74×10^3
benzyl alcohol	4.0	14.2×10^3

[a] Directly measured rate constants for reactions of $Fe(H_2O)_5O^{2+}$ in 0.1 M aqueous $HClO_4$.

Table 6. Products Obtained in Competition Between Protiated and Deuterated Substrates[a]

O_3 (mM)	substrate (mM)	product (mM)
1.15	diethyl ether-d_{10} (5.6)	acetaldehyde/ethanol (0.20)[b]
	benzyl alcohol (4.8)	benzaldehyde (0.66)
1.1	ethanol (16.6)	acetaldehyde (0.53)
	benzyl alcohol-d_2 (4.7)	benzaldehyde (0.18)
0.85	2-propanol-d_1 (10.1)	acetone (0.19)
	benzyl alcohol (4.8)	benzaldehyde (0.46)
1.39	cyclobutanol (9.7)	cyclobutanone (0.81)
	benzyl alcohol-d_2 (9.1)	benzaldehyde (0.34)
1	2-propanol-d_8 (10.3)	acetone (0.22)[b]
	benzyl alcohol (4.8)	benzaldehyde (0.54)

[a] By ^1H NMR. [b] Estimated from an experimentally determined amount of PhCHO and assuming a 75% cumulative yield of all products (as found with protiated substrates).

Table 7. Kinetic Isotope Effects for Reactions of $Fe^{IV}_{AN}O^{2+}$

substrate	k_H/k_D
diethyl ether (d_{10})	2.3
benzyl alcohol (d_2)	3.8
2-propanol (d_1, d_8)	2.5

All of the rate constants were normalized to k_{EtOH} = 1.0 in Table 5. Similar experiments with deuterated substrates (Figures S17−S21) yielded the results in Table 6, from which the kinetic isotope effects in Table 7 were calculated.

DOI: 10.1021/cs501962m
ACS Catal. 2015, 5, 1629−1637

DISCUSSION

The oxidation of alcohols, ethers, and sulfoxides by ozone in acetonitrile is catalyzed by $Fe(CH_3CN)_6^{2+}$. Concentrations of $Fe(CH_3CN)_6^{2+}$ as low as 0.02 mM are sufficient for the catalytic reaction to dominate over the uncatalyzed O_3/substrate reaction at substrate concentrations lower than ~50 mM. The catalyst not only provides rate acceleration but also increases the selectivity toward the less oxidized product. This is illustrated in Figure 1 and Figure S2 using the example of benzyl alcohol, which is oxidized to benzaldehyde in the $Fe(CH_3CN)_6^{2+}$-catalyzed path, and to a 1:1 mixture of benzaldehyde and benzoic acid in direct oxidation with ozone.

Saturation kinetics are observed at [substrate] > 5 mM (Figure 4). The rate constants reach an approximate limit of $k_{cat} = (8 \pm 1) \times 10^4\ M^{-1}\ s^{-1}$ for all of the substrates except diethyl ether, which reacts somewhat more slowly, $k_{cat} = (5 \pm 0.5) \times 10^4\ M^{-1}\ s^{-1}$. The observed variations in k_{cat} can be rationalized by variations in Fe(II)-substrate binding constants and perhaps different contributions from 1-e and 2-e paths (see below). The role of substrate binding is clearly seen in the reaction with DMSO, which interacts strongly with $Fe(CH_3CN)_6^{2+}$ and reaches $k_{cat} = 1.5 \times 10^6\ M^{-1}\ s^{-1}$ (Figure 5).

As the concentration of substrate drops below 5 mM, the rate constant decreases sharply (Figure 4). In this regime, up to 50% of iron is oxidized to Fe(III) in the course of the reaction, resulting in slower kinetics. Side reactions of Fe(IV) with $Fe(CH_3CN)_6^{2+}$ and with the solvent (see below) are also most severe at low substrate concentrations, which further reduces the efficiency of the catalytic reaction. The remainder of the discussion will focus on the saturation regime.

Most efficient are the oxidations of diethyl ether and dimethyl sulfoxide. Both generate 2-electron oxidation products quantitatively (Figures S5 and S6) with only small losses (≤20%) of the catalyst over 20−70 catalytic cycles (Table 1). These data are most easily explained by a single-step two-electron oxidation of substrates by $Fe^{IV}_{AN}O^{2+}$ (eq 6), followed by regeneration of $Fe^{IV}_{AN}O^{2+}$ in reaction 5.

Product yields are somewhat lower, 70−85%, in the reactions with alcohols (Table 1). We attribute these results to a contribution from a one-electron path of eq 8, which leads to oxygen radicals ($HO^\bullet/O^{\bullet-}$, $O_3^{\bullet-}$, $O_2^{\bullet-}$, and others) known to be involved in chain decomposition of O_3 in aqueous solutions.[19−24] Some of the key reactions believed responsible for the loss of O_3 in this work are shown in eqs 9−19, written in analogy with the chemistry in aqueous solutions and in the gas phase and supported by limited information on the reactivity of ozone and oxygen radicals in nonaqueous solvents.[25−30] The reaction of Fe(III) with hydroxyalkyl radicals was not considered in light of the much larger concentrations of the more reactive O_2 and O_3. In addition, there is no reaction between $Fe(CH_3CN)_6^{2+}$ and O_2 or with traces of H_2O_2 on the time scale of our experiments.

$$Fe^{IV}_{AN}O^{2+} + RCH_2OH \rightarrow Fe(III) + RC^\bullet HOH \quad (8)$$

$$RC^\bullet HOH + O_2 \rightarrow RCH(OH)OO^\bullet \quad (9)$$

$$RCH(OH)OO^\bullet \rightarrow RCHO + HO_2^\bullet/O_2^{\bullet-} \quad (10)$$

$$2RCH(OH)OO^\bullet \rightarrow \rightarrow \{2RCHO + O_2 + H_2O_2\} \xrightarrow{Fe(IV)} HO_2^\bullet + Fe(III) \quad (11)$$

$$RC^\bullet HOH + O_3 \rightarrow \rightarrow RC(O)OH + HO_2^\bullet/O_2^{\bullet-} \quad (12)$$

$$HO_2^\bullet \rightleftarrows O_2^{\bullet-} + H^+ \quad (13)$$

$$O_2^{\bullet-} + Fe(III) \rightarrow O_2 + Fe(II) \quad (14)$$

$$O_2^{\bullet-} + O_3 \rightarrow O_2 + O_3^{\bullet-} \quad (15)$$

$$O_3^{\bullet-} \rightleftarrows O^{\bullet-} + O_2 \quad (16)$$

$$O^{\bullet-} + H^+ \rightleftarrows HO^\bullet \quad (17)$$

$$(HO^\bullet, O_3^{\bullet-}, O^{\bullet-}) + CH_3CN(+O_2, O_3) \rightarrow \text{products} \quad (18)$$

$$(HO^\bullet, O_3^{\bullet-}, O^{\bullet-}) + RCH_2OH \rightarrow RC^\bullet HOH + (O_2, H_2O, HO^-) \quad (19)$$

Hydroxyalkyl radicals generated in eq 8 react with both O_2 (eq 9) and O_3 (eq 12) and produce superoxide, a powerful reductant and nucleophile.[30] The reduction of Fe(III) by $O_2^{\bullet-}$[24] (eq 14) is the key step that regenerates Fe(II). The competing reaction between O_3 and $O_2^{\bullet-}$,[31] the latter a well-recognized chain carrier in the decomposition of ozone,[23,32] generates $O_3^{\bullet-}$ followed by dissociation[33] to give $O^{\bullet-}$ (eqs 15, 16). The latter may be protonated (pK_a of $HO^\bullet$ in H_2O = 11.9)[34] if a sufficient amount of water is present in the solvent, but protonation is not required for the next step because both $HO^\bullet$ and $O^{\bullet-}$ will oxidize the solvent or substrate by hydrogen atom abstraction[33] (eqs 18, 19). Even though the rate constant for the reaction of $HO^\bullet$ with acetonitrile is smaller ($k = 1.0 \times 10^6\ M^{-1}\ s^{-1}$ in acetonitrile)[35] than the rate constants for the reactions with alcohols (e.g., $k_{EtOH} = 8.3 \times 10^7\ M^{-1}\ s^{-1}$),[26] the concentration advantage makes the reaction with CH_3CN about 5−10 fold faster at 20−50 mM ethanol that is typical in this work. Presumably, other radicals in eqs 18 and 19 exhibit a similar reactivity pattern and, together with $HO^\bullet$, lead to a loss of oxidizing equivalents and less than quantitative yields of substrate-derived products. Reaction 19 regenerates $RC^\bullet HOH$, which reenters the scheme.

According to the above mechanism, the beneficial effect of added Fe(III) arises mainly from its efficient scavenging of $O_2^{\bullet-}$ in eq 14.[24] This step both regenerates the catalyst and minimizes the importance of reactions 15−18 which lead to the loss of O_3.

Increased product yields and somewhat slower kinetics of O_3 loss under O_2-rich conditions are also consistent with known reactivity of radicals with O_3 and O_2. At high [O_2], most of the radicals react with O_2 as in eq 9, followed by reactions 10 and 11 and 13−19. In the absence of externally added O_2, the concentrations of O_2 and O_3 are comparable (see the Experimental Section), and reaction 12 becomes competitive with reaction 9, which increases the rate of ozone consumption and yields of doubly oxidized products.[36] Moreover, alkylperoxyl radicals produced in eq 9 also react with O_3 to generate alkoxyl radicals $RCH(OH)O^\bullet$ (eq 20), followed by rearrangement or further reactions with O_2, O_3, and substrates.[37,38]

$$RCH(OH)OO^\bullet + O_3 \xrightarrow{-O_2} RCH(OH)O^\bullet \xrightarrow{O_2, O_3, \text{substrate}} \text{products} \quad (20)$$

In agreement with the above scheme, the concentration of O_2 found after completion of the reactions with alcohols is significantly smaller than one would calculate by adding the

DOI: 10.1021/cs501962m
ACS Catal. 2015, 5, 1629−1637

amount produced from ozone in reaction 5 to the $[O_2]$ initially present. Clearly, some O_2 is consumed in the course of alcohol oxidation. On the other hand, the concentration of O_2 found after the oxidation of DMSO and $(C_2H_5)_2O$ is close to that calculated, supporting the notion that 1-e oxidation of these substrates is negligible. DMSO is probably oxidized by OAT, similar to the reaction in water.[1] Quantitative product yields and measurable hydrogen kie for diethyl ether suggests hydride transfer.[1] Additional support for hydride transfer comes from the effect of alcohols on oxidation products of THF. The formation of acetals is most reasonably explained by hydride transfer that generates an oxonium ion, followed by the reaction with alcohols, as shown in Scheme 2. The oxonium ion shown was proposed earlier as an intermediate in cationic polymerization of THF in the presence of triphenylmethyl cation salts.[39]

Scheme 2. Mechanism for THF Oxidation by Hydride Transfer to $Fe(CH_3CN)_5O^{2+}$

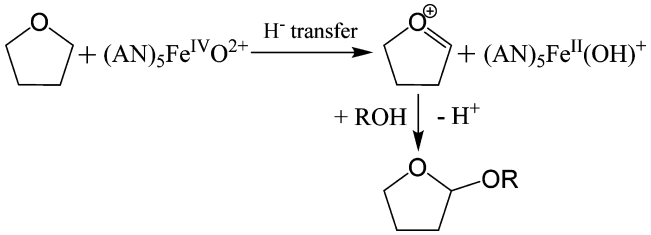

The alternative rebound mechanism that begins with hydrogen atom transfer would generate the hemiacetal, as shown in Scheme 3. This mechanism is ruled out by our

Scheme 3. Mechanism for THF Oxidation by Hydrogen Atom Transfer to $Fe(CH_3CN)_5O^{2+}$

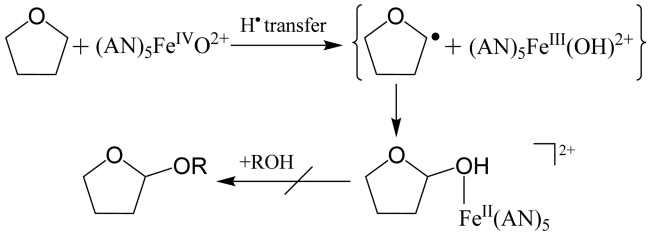

observation that the hemiacetal does not react with alcohols under our conditions. In contrast with ethers, the intermediates generated in the process of alcohol oxidation by hydride transfer generate aldehydes/ketones by rapid deprotonation at oxygen.

The induction period observed in the O_3/substrate reaction when iron is initially present as Fe(III) is most easily explained by the need to reduce Fe(III) to Fe(II), presumably through a scheme involving one-electron reduction of O_3 by substrate,[19,40,41] followed by eqs 16−19. The complex, multistep chemistry in eqs 18 and 19 is envisioned to generate some $O_2^{\bullet-}$, which reduces Fe(III) to Fe(II) and thus leads to the production of $Fe^{IV}_{AN}O^{2+}$ via reaction 5. Another possibility is a slow, direct oxidation of Fe(III) by ozone to generate high oxidation state iron species[42] that would be rapidly reduced to Fe(II).

The disappearance of ozone in the presence of catalytic amounts of $Fe(CH_3CN)_6^{2+}$ in acetonitrile, even in the absence of more reducing substrates, shows that the solvent itself can be catalytically oxidized. It is not clear whether $Fe^{IV}_{AN}O^{2+}$ oxidizes CH_3CN in 1-e or 2-e steps. Measurable amounts of $Fe(CH_3CN)_6^{2+}$ found in such solutions after all of the O_3 disappeared support a 2-e catalytic reaction that might take place by oxygen atom transfer or hydride transfer. On the other hand, as shown above in the reaction with alcohols, 1-e chemistry can also bring about the disappearance of ozone and formation of $Fe(CH_3CN)_6^{2+}$. In support of one-electron route, we note that aqueous $Fe^{IV}_{aq}O^{2+}$ reacts with CH_3CN by hydrogen abstraction and does not regenerate Fe_{aq}^{2+}.[1] In addition, the much smaller amount of recovered Fe(II) after completion of Fe(II)/O_3 reaction in CD_3CN indicates a large solvent isotope effect, again consistent with HAT, although hydride abstraction cannot be entirely ruled out.

Throughout this discussion, it has been assumed that the oxidizing intermediate is an Fe(IV) species, $Fe^{IV}_{AN}O^{2+}$, although so far, we have not been able to observe or characterize it spectroscopically. This assignment is made in analogy to the results in aqueous solution, where the product of $Fe(H_2O)_6^{2+}$/O_3 reaction has been identified as $Fe_{aq}O^{2+}$,[1,2] and at interfaces with chloride-containing solutions where $O{=}Fe^{IV}Cl_3^-$ is generated.[43] The relative reactivity toward substrates in Table 5 appears consistent with this assignment in that the trend in acetonitrile follows closely that observed for $Fe_{aq}O^{2+}$ in aqueous solutions. In that work, it was possible to carry out direct kinetic measurements of substrate oxidation by preformed $Fe_{aq}O^{2+}$. As shown in Table 5, benzyl alcohol is the most reactive among alcohols in both solvents, but the yield of 2-e oxidation product in acetonitrile is among the lowest. This result may suggest a significant contribution from the 1-e path. Alternatively, the reaction may involve an attack by $Fe^{IV}_{AN}O^{2+}$ at the aromatic ring to generate multiple products, similar to the reaction of O_3 with $PhCH_2OH$,[44] or reactions of other Fe(IV)-oxo complexes with aromatic compounds.[45,46]

The kinetic isotope effect for the reaction with 2-propanol is also similar in the two solvents. The value of k_H/k_D for the methine C−H is 2.5 in acetonitrile (Table 7) and 2.1 in H_2O,[1] consistent with the hydride transfer proposed previously. These results, however, do not rigorously rule out other potential oxidizing intermediates, such as an ozonide or Fe(III)−(CH_2CN) radical that may also react by hydride or hydrogen atom transfer.

CONCLUSIONS

Perchlorate and trifluoromethanesulfonate salts of iron(II) efficiently catalyze the oxidation of alcohols and ethers with ozone in acetonitrile. This result stands in stark contrast with that obtained in acidic aqueous solutions where, under comparable conditions, all of $Fe(H_2O)_6^{2+}$ is quickly oxidized to the unreactive $Fe(H_2O)_6^{3+}$.

The difference between the two solvents can be rationalized by changes in redox thermodynamics of iron and acid−base chemistry of superoxide, $HO_2^{\bullet}/O_2^{\bullet-}$, as follows: In both solvents, the reaction between the substrate and active oxidant, an iron(IV) species, takes place in parallel one-electron (hydrogen-atom abstraction) and two-electron (hydride transfer) paths. The two-electron path is much more prominent in acetonitrile, presumably because it avoids the strongly oxidizing Fe(III) (E = 1.6 V vs NHE).[8] This path regenerates the active catalyst, $Fe(CH_3CN)_6^{2+}$, directly. The minor parallel hydrogen atom transfer path produces carbon radicals and Fe(III), followed by radical/O_2 reaction that generates superoxide

DOI: 10.1021/cs501962m
ACS Catal. 2015, 5, 1629−1637

($E^0(O_2/O_2^{\bullet-})$ = −0.80 V vs NHE).[30] The rapid reaction of $O_2^{\bullet-}$ with Fe(III) regenerates the catalyst and removes $O_2^{\bullet-}$, the key intermediate involved in chain decomposition of ozone.

The two paths are of comparable importance in acidic aqueous solutions[1] so that a substantial portion of $Fe(H_2O)_6^{2+}$ is oxidized to $Fe(H_2O)_6^{3+}$ in a single cycle. Similar to the reaction in acetonitrile, the radical/O_2 chemistry generates superoxide, but this intermediate is rapidly protonated under the acidic conditions employed (pK_a ($HO_2^{\bullet}$/ $O_2^{\bullet-}$) = 4.69).[30] The protonation prevents the superoxide from reducing $Fe(H_2O)_6^{3+}$ and regenerating the catalyst.

■ ASSOCIATED CONTENT

Supporting Information

The following file is available free of charge on the ACS Publications website at DOI: 10.1021/cs501962m.

Figures S1−S21 and Tables S1−S3 (PDF)

■ AUTHOR INFORMATION

Corresponding Authors

*E-mail: pvp@iastate.edu.
*E-mail: bakac@iastate.edu

Notes

The authors declare no competing financial interest.

■ ACKNOWLEDGMENTS

We are grateful to Dr. Jana for help with the synthesis of iron(II) bis(acetonitrile) complex. This research is supported by the U.S. Department of Energy, Office of Science, Basic Energy Sciences, Division of Chemical Sciences, Geosciences, and Biosciences through the Ames Laboratory. The Ames Laboratory is operated for the U.S. Department of Energy by Iowa State University under Contract DE-AC02-07CH11358.

■ REFERENCES

(1) Pestovsky, O.; Bakac, A. *J. Am. Chem. Soc.* **2004**, *126*, 13757−13764.
(2) Pestovsky, O.; Stoian, S.; Bominaar, E. L.; Shan, X.; Münck, E.; Que, L. J.; Bakac, A. *Angew. Chem., Int. Ed.* **2005**, *44*, 6871−6874.
(3) Jacobsen, F.; Holcman, J.; Sehested, K. *Int. J. Chem. Kinet.* **1998**, *30*, 215−221.
(4) Logager, T.; Holcman, J.; Sehested, K.; Pedersen, T. *Inorg. Chem.* **1992**, *31*, 3523−3529.
(5) Pestovsky, O.; Bakac, A. *Inorg. Chem.* **2006**, *45*, 814−820.
(6) Bataineh, H.; Pestovsky, O.; Bakac, A. *Chem. Sci.* **2012**, *3*, 1594−1599.
(7) Kratochvil, B.; Long, R. *Anal. Chem.* **1970**, *42*, 43−46.
(8) Sugimoto, H.; Sawyer, D. T. *J. Am. Chem. Soc.* **1985**, *107*, 5712−5716.
(9) Bakac, A.; Pestovsky, O.; U.S. Patent 8507730, 2013.
(10) Hagen, K. S. *Inorg. Chem.* **2000**, *39*, 5867−5869.
(11) Leitzke, A.; von Sonntag, C. *Ozone: Sci. Eng.* **2009**, *31*, 301−308.
(12) Franco, C.; Olmsted, J., III *Talanta* **1990**, *37*, 905−909.
(13) Nimlos, M. R.; Wolfrum, E. J.; Brewer, M. L.; Fennell, J. A.; Bintner, G. *Environ. Sci. Technol.* **1996**, *30*, 3102−3110.
(14) Hay, M. T.; Geib, S. J.; Pettner, D. A. *Polyhedron* **2009**, *28*, 2183−2186.
(15) Avgousti, C.; Georgolios, N.; Kyriacou, G.; Ritzoulis, G. *Electrochim. Acta* **1999**, *44*, 3295−3301.
(16) Klang, J. A.; Lawson, A. P.: United States, 1993; US005254702A, p 1−4.
(17) Suárez, A. R.; Rossi, L. I.; Martín, S. E. *Tetrahedron Lett.* **1995**, *36*, 1201−1204.
(18) Kirchner, K.; Kirchner, R.; Jedlicka, R.; Schmid. *Monatsh. Chem.* **1992**, *123*, 203−209.
(19) Flyunt, R.; Leitzke, A.; Mark, G.; Mvula, E.; Reisz, E.; Schick, R.; von Sonntag, C. *J. Phys. Chem. B* **2003**, *107*, 7242−7253.
(20) Langlais, B.; Reckhow, D. A.; Brink, D. R. In *American Water Works Research*; CRC press: Boca Raton, FL, 1991.
(21) Gonzalez, M. C.; Mártire, D. O. *Int. J. Chem. Kinet.* **1997**, *29*, 589−597.
(22) Gonzalez, M. C.; Mártire, D. O. *Water Sci. Technol.* **1997**, *35*, 49−55.
(23) Naumov, S.; von Sonntag, C. *Environ. Sci. Technol.* **2011**, *45*, 9195−9204.
(24) Rush, J. D.; Bielski, B. H. J. *J. Phys. Chem.* **1985**, *89*, 5062−5066.
(25) Nakano, Y.; Okawa, K.; Nishijima, W.; Okada, M. *Water Res.* **2003**, *37*, 2595−2598.
(26) Mitroka, S.; Zimmeck, S.; Troya, D.; Tanko, J. M. *J. Am. Chem. Soc.* **2010**, *132*, 2907−2913.
(27) Afanas'ev, I. B.; Kuprianova, N. S. *J. Chem. Soc., Perkin Trans. 2* **1985**, 1361−1364.
(28) Singh, P. S.; Evans, D. H. *J. Phys. Chem. B* **2005**, *110*, 637−644.
(29) McCandlish, E.; Miksztal, A. R.; Nappa, M.; Sprenger, A. Q.; Valentine, J. S.; Stong, J. D.; Spiro, T. G. *J. Am. Chem. Soc.* **1980**, *102*, 4268−4271.
(30) Sawyer, D. T.; Valentine, J. S. *Acc. Chem. Res.* **1981**, *14*, 393−400.
(31) Bielski, B. H. J.; Cabelli, D. E.; Arudi, R. L.; Ross, A. B. *J. Phys. Chem. Ref. Data* **1985**, *14*, 1041−1100.
(32) Lind, J.; Merenyi, G.; Johansson, E.; Brinck, T. *J. Phys. Chem. A* **2003**, *107*, 676−681.
(33) Gall, B. L.; Dorfman, L. M. *J. Am. Chem. Soc.* **1969**, *91*, 2199−2204.
(34) Buxton, G. V.; Greenstock, C. L.; Helman, W. P.; Ross, A. B. *J. Phys. Chem. Ref. Data* **1988**, *17*, 513−886.
(35) DeMatteo, M. P.; Poole, J. S.; Shi, X.; Sachdeva, R.; Hatcher, P. G.; Hadad, C. M.; Platz, M. S. *J. Am. Chem. Soc.* **2005**, *127*, 7094−7109.
(36) Sehested, K.; Holcman, J.; Bjergbakke, E.; Hart, E. J. *J. Phys. Chem.* **1987**, *91*, 2359−2361.
(37) Batt, L. *Int. Rev. Phys. Chem.* **1987**, *6*, 53−90.
(38) Kirillov, A. I. *Zh. Obshch. Khim.* **1966**, *2*, 1048−1052.
(39) Kuntz, I. *J. Polym. Sci., Part B: Polym. Lett.* **1966**, *4*, 427−430.
(40) Martín, S. E.; Suárez, D. o. F. *Tetrahedon Lett.* **2002**, *43*, 4475−4479.
(41) Hellman, T. M.; Hamilton, G. A. *J. Am. Chem. Soc.* **1974**, *96*, 1530−1535.
(42) Gross, Z.; Simkhovich, L. *J. Mol. Catal. A: Chem.* **1997**, *117*, 243−248.
(43) Enami, S.; Sakamoto, Y.; Colussi, A. J. *Proc. Natl. Acad. Sci. U.S.A.* **2013**, *111*, 623−628.
(44) Potapenko, E. V.; Andreev, P. Y. *Russ. J. Appl. Chem.* **2010**, *83*, 1243−1247.
(45) Fitzpatrick, P. F. *Biochemistry* **2003**, *42*, 14083−14091.
(46) de Visser, S. P.; Oh, K.; Han, A.-R.; Nam, W. *Inorg. Chem.* **2007**, *46*, 4632−4641.

DOI: 10.1021/cs501962m
ACS Catal. 2015, 5, 1629−1637